Optimization of Control Strategies for the Radiant Floor Cooling System Combined with Displacement Ventilation: A Case study of an Office Building in Jinan, China

Jiying Liu[1,*], Jing Ren[1], Linfang Zhang[1], Xiaona Xie[1], Moon Keun Kim[2] and Linhua Zhang[1,3]

[1]*School of Thermal Engineering, Shandong Jianzhu University, Jinan 250101, China*

[2]*Department of Architecture, Xi'an Jiaotong-Liverpool University, Suzhou 215123, China*

[3]*Shandong Province Green Building Collaborative Innovation Center, Shandong Jianzhu University, Jinan 250101, China*

Abstract: The radiant floor cooling system, as a thermally activated building system, has attracted significant attention as it can save energy consumption and shift the building load. However, due to its characteristic that building thermal mass has a significant influence on the system performance and indoor environment, the control strategies should be seriously accounted for. Moreover, its performance is highly related to the shift condition of cooling load during the daytime and different weather conditions, therefore, realistic operation will cause the increments of peak load if the control strategy is neglected. This study presented two common strategies including intermittent operation and weather-forecast-based control strategies. The radiant floor cooling system combined with displacement ventilation system in a typical office building located in Jinan was established using the TRNSYS program. The results showed that the energy consumption decreased by 3.3% to 7.5% when the different intermittent operation strategies were applied. The weather-forecast-based control strategy can improve indoor thermal environment by increasing/deceasing the water supply flow rate by up to 25% in advance. This study concluded that the application of intermittent operation and weather-forecast-based control strategies can regulate the operation of radiant floor system and reduce the building energy use.

Keywords: Radiant floor cooling system, displacement ventilation, TRNSYS, control strategy, indoor environment.

INTRODUCTION

With the improvement of the living environment and the development of urbanization [1-4], building energy consumption in urban areas is rapidly increasing [5-7]. Therefore, developing a low-carbon economic development mode and renewable energy is the effective way to solve the problem of energy shortages [8]. At present, the main task in the study of air conditioning energy consumption is to optimize air conditioning systems to reduce energy consumption, and improve comfort and encourage the use of renewable energy. Solar energy can be greatly influenced by meteorological conditions, while geothermal energy, which provides cooling and heating sources, is currently widely used due to its better stability. A ground source heat pump (GSHP) system can accomplish the transformation from low-quality energy to high-quality energy [9], which is presented as a technology that can fully supply the heating, ventilation and air conditioning (HVAC) conditions for a building and can be environmentally friendly [10]. A promising technology, for example, thermal energy storage, is considered to improve the energy consumption level of building HVAC system, if incorporated in the building envelope, the energy consumption can be reduced [11, 12]. Therefore, thermal mass is beneficial for maintaining indoor thermal comfort and saving energy [13-15]. The floor radiant air-conditioning system adopts the inert concrete radiant terminal and has better heat storage (cold) characteristics and thermal comfort [16], which provides the possibility of using natural cooling and heating sources [17]. The system can be used both in winter and summer seasons with the same set of water pipes, saving investment in the air-conditioning system and building space [18].

There have been extensive studies into radiant air-conditioning systems [19-22]. Ning *et al*. [23] pointed out that concrete thickness, pipe spacing, and concrete properties significantly affected on the response time of thermally activated building systems. Sourbron *et al*. [24] indicated that the envelope of a radiant air-conditioning system has an energy storage capacity. Lehmann *et al*. [25] adopted the pulse control method to implement the intermittent control of air-conditioning systems, and used the trough electricity price time to store energy. Cen *et al*. [26] concluded that a fan–coil system would cause a higher temperature at the activity sites of people in tall buildings, while floor radiant air-conditioning systems should be adopted. A review study concluded that most of existing control models are limited to real-time controls, for example,

*Address correspondence to this author at the School of Thermal Engineering, Shandong Jianzhu University, Jinan 250101, China; Tel: 86-531-86361236; Fax: 86-531-86361236; E-mail: jxl83@sdjzu.edu.cn, j.y.liu@hotmail.com

E-ISSN: 2409-9821/19

on/off criteria [27-29]. Shin *et al*. [30] determined the optimal heating start and stop control based on the occupancy schedules to improve energy saving performance and thermal comfort. Lim *et al*. [31] investigated that controlling the supply water temperature and on/off instead of water flow rate can be the main control strategies to prevent the floor surface condensation in hot and humid weather conditions. It should be noted that the application of a floor radiant heating system in winter is quite common, but the application range of floor radiant cooling system is limited due to its own disadvantages [32], for example, underdeveloped operation techniques, easy condensation characteristic, and immature control strategy. Moreover, the system's performance is highly related to the shift condition of cooling load during the daytime and different weather conditions, therefore, realistic operation will cause the increments of peak load if the control strategy is neglected. Therefore, it is necessary to explore the control mode of radiant air-conditioning systems, which is conducive to the application of this comfortable and energy-saving system.

The main purpose of this study was to propose two control strategies of floor radiant cooling system to improve indoor thermal environment, which include intermittent operation and weather-forecast-based predictive control strategies. The study was established by conducting a radiant floor cooling system (RFCS) combined with a displacement ventilation (DV) system in a typical office building in Jinan using the TRNSYS program. The intermittent operation control strategy took into account the system operation schedule by changing the water supply flow rate and air fan flow rate during weekends. The weather-forecast-based predictive control strategy mainly considered the situations of high-temperature weather and rainy weather. Correspondingly, the variations of indoor equipment and occupancy were also analyzed, where the increase or decrease of cooling load exceeded a certain limitation value. Meanwhile, the indoor air temperature, relative humidity, and energy consumption were compared under different operation strategies. The optimum water supply and air supply flow rate measures were finally obtained to improve the performance of the RFCS–DV system.

Introduction of a Coupled RFCS–DV System

This study utilized the Shandong Antaeus dynamic energy-saving demonstration building located in the cold climate zone in Jinan, China [33, 34]. This building had a floor area of 5400 m^2, with a ground area of 4580 m^2 and underground area of 820 m^2. The building adopts a GSHP system with displacement ventilation system, as shown in Figure **1**. This system had a total of 56 boreholes with a depth of 100 meters each distributed around the building. Note that the exclusive energy-consuming equipment was the direct cooling circulating pump, which directly draws circulating water to floor piping with the temperature of about 18°C. In the cooling season, the sensible heat load was removed by the radiant floor cooling system by directly utilizing. This system was called as ground source direct cooling system (GSDC) in this study.

The most of the sensible heat load was undertook by floor cooling part, directly utilizing the high-temperature cold water from buried U-shape tubes, while the DV system, as a commonly used ventilation system [35, 36], bears all the latent heat load and the possible sensible heat load by using 7°C chilled water stored in a water tank in a valley power period. In the heating season, the system adopts the electric rate difference to generate lower-temperature hot water if

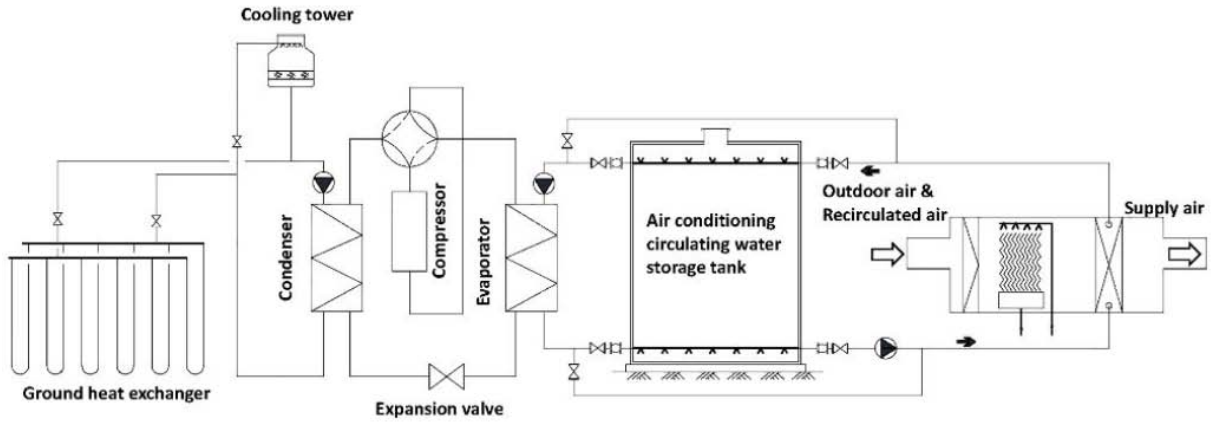

Figure 1: Schematic drawing of GSDC and DV system [33].

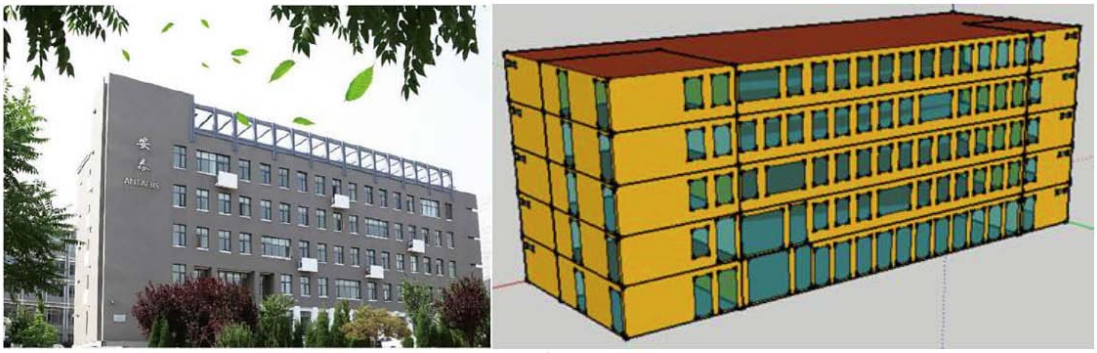

(a) (b)

Figure 2: Side view for the Shandong Antaeus energy-saving demonstration building, (**a**) Realistic building [33], (**b**) Simulation model.

necessary. The combination of GSDC and DV system cools and dehumidifies the outdoor air entering through the cooling coil in the ventilator by lowering the dew-point temperature to prevent condensation on the floor surface. In terms of thermal comfort, the combined system achieves high scores, ensuring comfort conditions during most of the cooling season.

ENERGY SIMULATION

Model Description for the Simulation Cases

A side view of the three-dimensional model of the Shandong Antaeus energy-saving demonstration building is shown in Figure **2**. The building energy simulation model and schedule setup are presented in Table **1** and Figure **3**, respectively.

Table 1: Building Energy Simulation Model Setup

People (m^2/per people)	1st floor 40.0 2nd floor 30.0 3rd floor 20.0 4th floor 30.0 5th floor 40.0
Equipment load (W/m^2)	1st floor 5.0 2nd floor 6.0 3rd floor 10.0 4th floor 8.0 5th floor 4.0
Lighting load (W/m^2)	10
Outdoor air rate (m^3/(h.per person))	30
Design temperature in summer (°C)	26
Design relative humidity in summer (%)	60

There are four layers under the floor in the RFCS, including the granite title cement mortar screed-coat, filling-in concrete layer containing the buried pipe, insulation layer, and reinforced concrete. Detailed thermal physical properties of the floor structures can be found in Table **2**. The parameters set up for buried pipes are presented in Table **3**. Figure **4** is the RFCS-DV simulation platform built by TRNSYS 17 [37].

Cooling Load Simulation

The cooling period of the office building was chosen from June 15 to September 15. The simulated cooling load of the building is presented in Figure **5**. In the radiant floor and cooling systems, solar radiation has a large influence on indoor air temperatures and the energy efficiency of the radiant system [38]. The results showed that the maximum load is 209 kW, including a sensible heat load of 172 kW and a latent heat load of 37 kW. The air conditioning cooling load is 55W/m^2. A part of the sensible heat load were borne by the DV system.

The HVAC design of the building considered a GSDC combined with RFCS and DV systems, which offers several advantages such as the ability for load shifting from daytime to night-time and reducing peak energy demand [39]. This system generates a good level of control with higher efficiency and quality [40]. Figure **6** shows the supply and return water temperature in the system. The water supply temperature ranges about 18~19°C, and the return water temperature ranges about 19.5~20.5 °C. The variation of supply and return temperature is small with relatively stable difference, which is the advantage of GSDC system for selecting the source of soil to cool and heat. Note that a constant supply water flow rate of 30000 kg/h was used as the reference in this study.

Energy Simulation Validation

The office building is equipped with building automation and control systems which control the

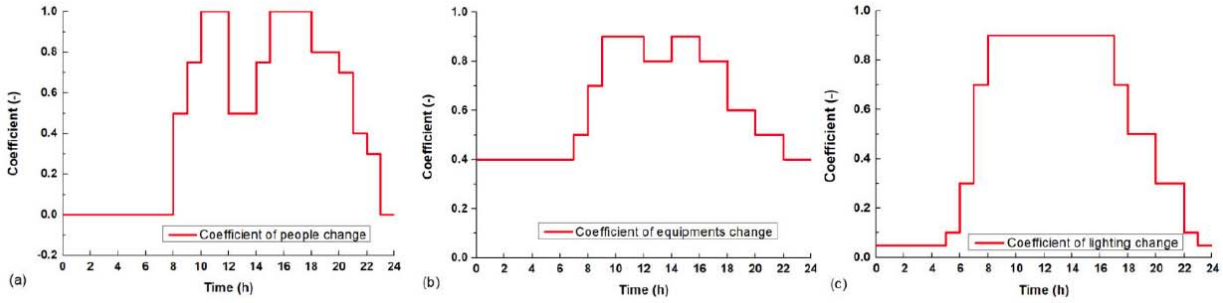

Figure 3: Schedules in the simulation model, (**a**) people, (**b**) equipment, (**c**) lighting.

Table 2: Thermal Physical Properties of the Floor Materials

Material	Thickness (mm)	Thermal conductivity (W/m·K)	Heat capacity (J/kg·K)	Density (kg/m^3)
Granite title	20	3.49	920	2800
Cement mortar screed-coat	10	3.35	1050	1800
Filling-in concrete layer	30	1.74	920	2500
Insulation layer	20	0.04	5380	25
Reinforced concrete	200	1.74	1000	1800

Table 3: Buried Pipe Parameters Set-Up

Specific heat coefficient of water (J/kg·K)	4180
Pipe spacing (m)	0.25
Pipe outer diameter (m)	0.025
Pipe wall thickness (m)	0.002
Pipe wall conductivity (W/m·K)	1.26

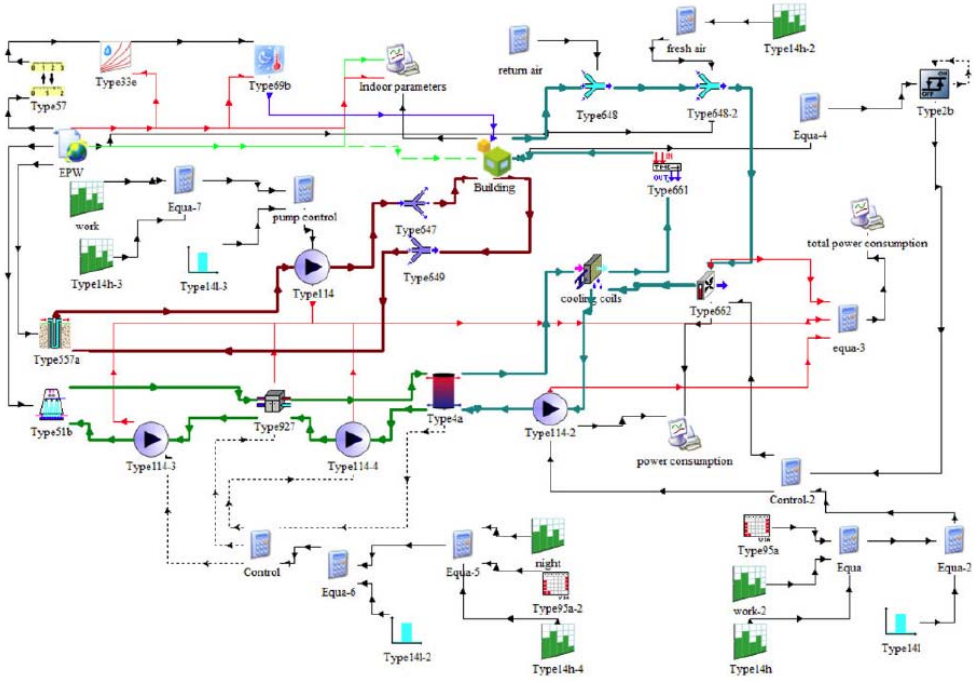

Figure 4: The simulation platform of the RFCS-DV in TRNSYS program.

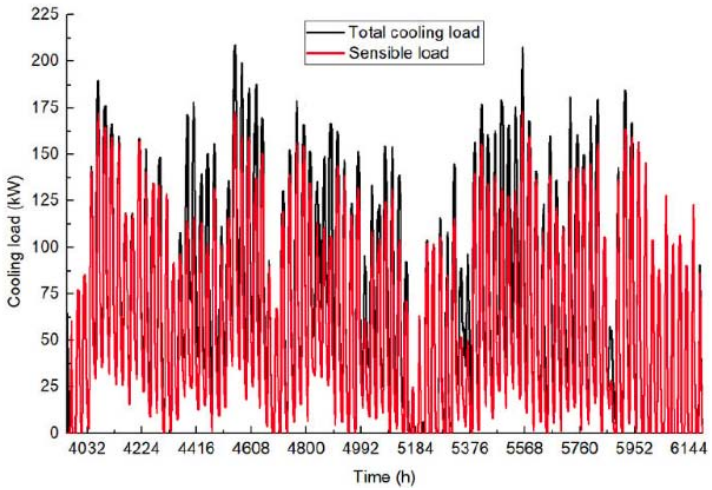

Figure 5: Result of the simulated cooling load from June 15 to September 15.

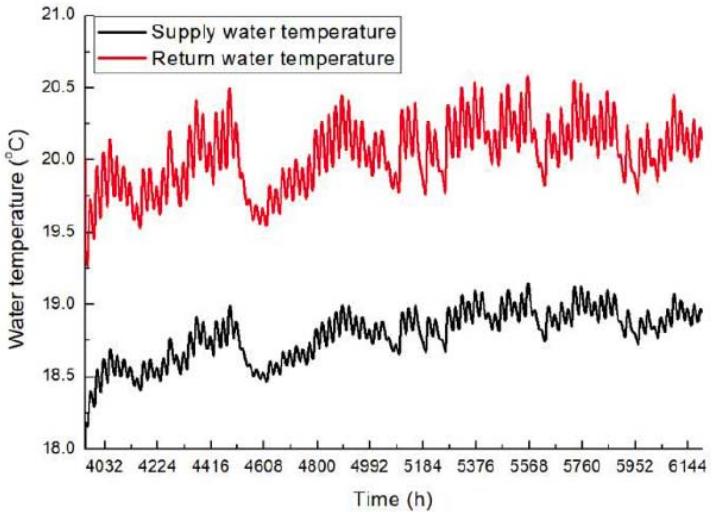

Figure 6: The water temperature of the GSDC system.

air-conditioning system and monitor the air-conditioning operation parameters, including the indoor air temperature and humidity and the electric power consumption of equipment, constantly. The monitoring system measures the indoor air temperature and humidity and transmits them to the temperature and humidity monitoring platform every 15 minutes. The experimental and simulated temperature of the third floor from July 1 to 8 are obtained. The comparison results are shown in Figure **7**.

It can be seen that the fluctuating range of the indoor air temperature is small at basically between 22.0 and 26.5, and the simulated indoor air temperature located with the similar ranges. There are some discrepancies between the simulated indoor air temperature and the measured data, but the majority relative error is basically controlled within 5%, which is acceptable. The main reason is that the number of indoor people and equipment load are fluctuating values that significantly affect the simulation results. The fixed value in a relatively large period in the energy simulation setup was used to create the simulation deviations.

Prediction of Outdoor Temperature and Solar Radiation

In the predictive control strategy, higher energy efficiency relies on good forecast of outdoor weather condition, especially in the day time [41]. The commonly used outdoor air temperature prediction methods include the MacArthur shape factor method [42] and ASHRAE coefficient method [43]. The ASHRAE coefficient method is selected in this study to predict the hourly outdoor air temperature, due to its simpler and fast characteristic. The summer season

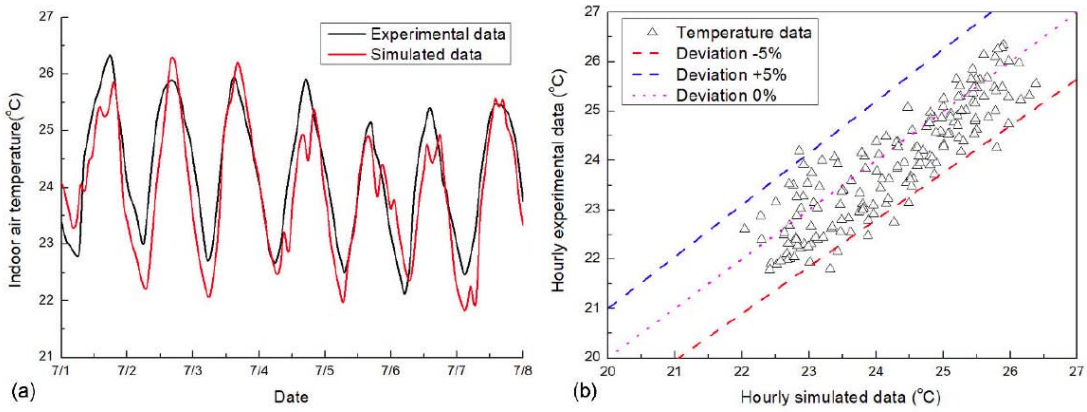

Figure 7: Indoor air temperature comparison (**a**) and deviation analysis (**b**) between experimental and simulated data from July 1 to 7.

from June 15 to September 15 was employed. The predicted outdoor air temperature results are shown in Figure **8**. It can be found that there are significant difference between those data. This study used the effective and convenient method, Kawashima method [44], to predict solar radiation. Figure **9** shows that the predicted solar radiation and typical annual meteorological solar radiation data is quite different.

INTERMITTENT OPERATION

Intermittent Operation of the GSDC System

The intermittent operation is determined by the heat gain from the floor heat storage and release [45]. The operation mode mainly takes advantage of the thermal inertia and energy storage of the concrete's radiant end

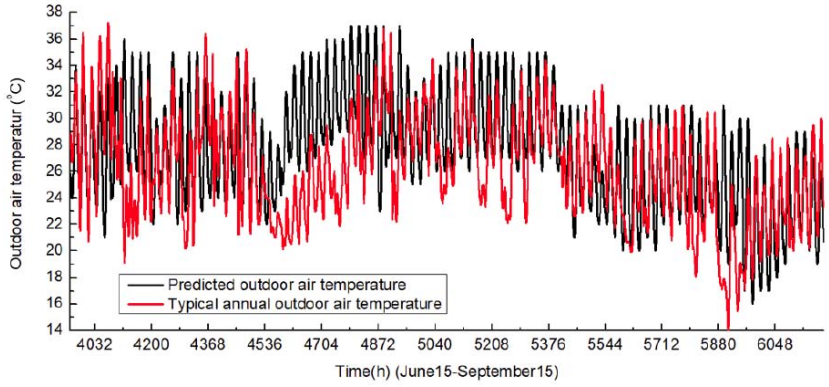

Figure 8: Simulated outdoor air temperature and typical annual outdoor air temperature.

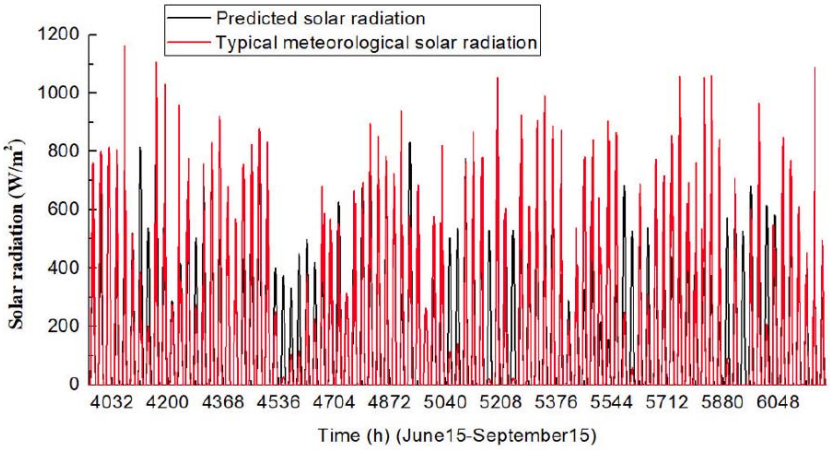

Figure 9: Typical meteorological year solar radiation and predicted solar radiation.

Table 4: Control Strategies of the GSDC System

Case	Modes
Case GSDC0	0:00–24:00 daily
Case GSDC1	8:00–18:00 daily
Case GSDC2	6:00–18:00 daily
Case GSDC3	5:00–18:00 daily
Case GSDC4	0:00–24:00 weekdays

[46]. Table **4** shows the five intermittent control schemes. Case GSDC0 is the basic case. Figure **10** shows the indoor air temperature comparisons. It can be seen that Case GSDC1, Case GSDC 2 and Case GSDC3 increased the indoor air temperature by 2~3˚C. And because Case GSDC4 operates continuously on weekdays, the variation of indoor air temperature is similar to that of Case GSDC0. The temperature of Case GSDC4 is significantly higher than that of Case GSDC0, mainly due to the closure of the system.

In radiant floor systems, the temperature of the floor surface determines the cooling/heating capacity and indoor thermal comfort [47]. The floor surface temperature comparisons are shown in Figure **11**. Most of the floor surface temperature of Case GSDC0 is between 20~22˚C. The temperatures of Case GSDC1, Case GSDC2 and Case GSDC3 are higher. The temperature of Case GSDC4 is about 1.0˚C higher than that of Case GSDC0 on weekdays, and the temperature is apparently higher on weekends, mainly because the GSDC system is closed on weekends. If there are no occupancy in the office building or if only

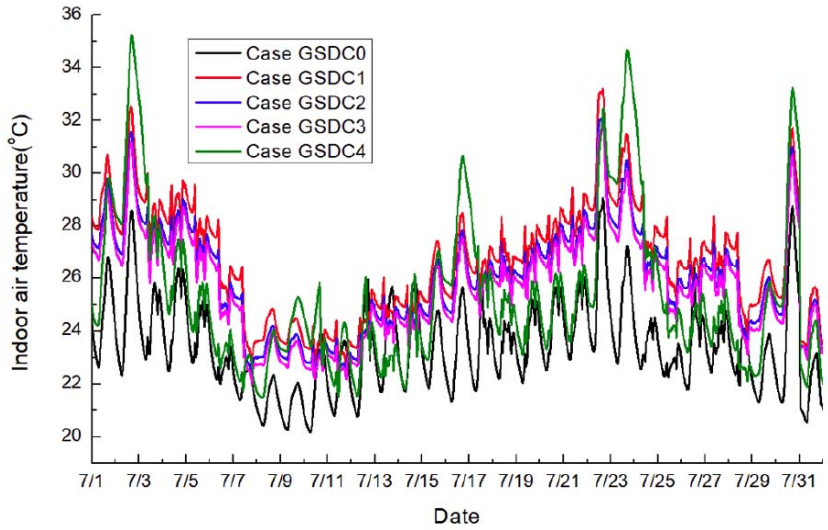

Figure 10: Indoor air temperature on the fifth floor in July.

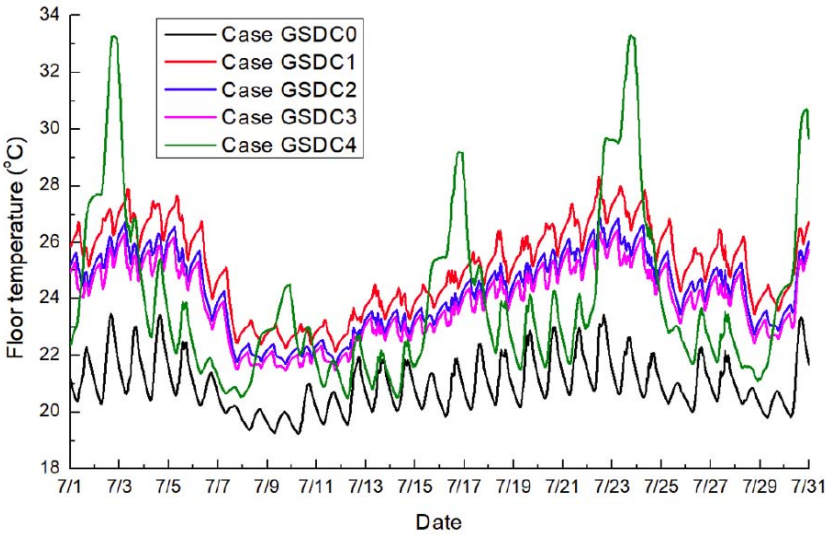

Figure 11: Floor surface temperature on the fifth floor in July.

some people are working on Saturdays and Sundays, Case GSDC4 can be used. Through the comparison between Case GSDC0 and Case GSDC4, it can be observed that a significant energy saving of 1426 kWh for a circulating water pump can be achieved for the whole cooling season.

Intermittent Operation of the DV System

The DV system has the purpose of removing the latent heat load and a part of the sensible heat load. Therefore, the intermittent operation for the DV system is characterised as remarkable variation of air humidity. Three control strategies are shown in Table **5**.

Table 5: Control Strategies of the DV System

Case	Running time
Case DV0	8:00–18:00 on weekdays
Case DV1	8:00–17:00 on weekdays
Case DV2	8:00–16:00 on weekdays

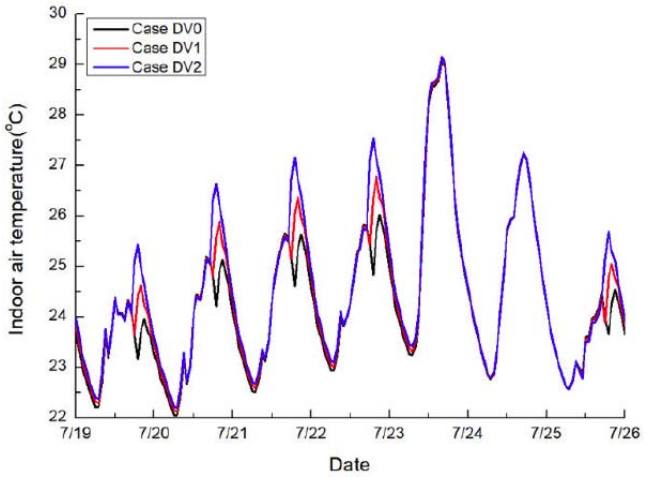

Figure 12: Comparison of indoor air temperature for DV system.

Figures **12** and **13** show the comparisons of indoor air temperature and air humidity from July 19 to 26. It can be seen that turning off the DV system in advance did not affect the air temperature too much. The indoor air temperature only increase by 0.2~0.3˚C which can be neglected. The maximum difference of air humidity reached up to 8%. Through turning off the dehumidifying one hour in advance, the relative humidity can increase by up to 3%. While the indoor relative humidity increased by up to 8% if two hours was considered. The maximum relative humidity exceeded 65% which will bring the risk of floor condensation. Therefore, turning off DV system one hour earlier has little effect on the condensation risk and was taken as the control case.

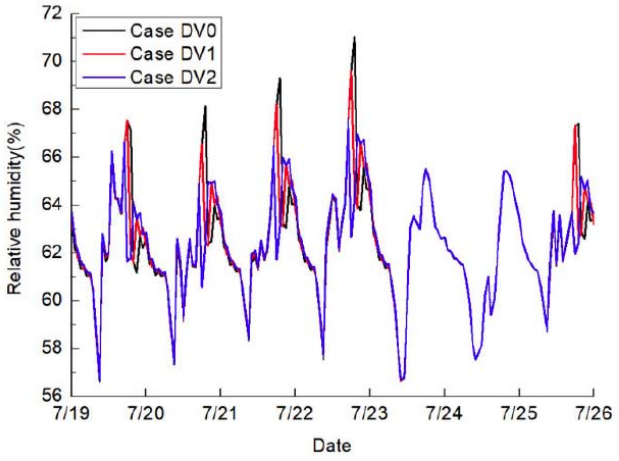

Figure 13: Comparison of indoor air humidity for DV system.

Choice of Control Strategies for Integrated GSDC and DV System

The combined plans of GSDC and DV are presented in Table **6**. Figures **14** and **15** showed the indoor air temperature and relative humidity distribution. The high temperature occurred on weekend and Monday for Case GSDC-DV1. The peak relative humidity increased during the entire cooling season, however, the maximum value is about 63%, which basically meets the control needs of indoor occupancy. In the end, the combined control strategy can be considered for buildings with low comfort requirements. Intermittent operation during the daytime had no significant effect on the indoor air temperature variation due to the response time, while it decreased energy consumption by up to 7.5% when the GSDC system operated on weekdays rather than the whole cooling season as shown in Table **7**.

Operation Strategies Affected by Equipment and Occupancy Changes

RSFC is commonly used in commercial buildings, mainly because of the highly constant occupancy level. However, when the number of people increases, the original control method may not be able to meet the cooling demand. A decrease of people will cause the waste of cooling capacity, resulting in a lower indoor air temperature, which may lead to thermal discomfort for people. In this section, the different cases with changes of the number of people and equipment load are shown in Table **8**.

Taking the fifth floor as an example for data analysis, Figure **16** shows the comparison of cooling

Table 6: Control Schedules of Combined GSDC and DV System

Case	GSDC system	DV system
Case GSDC-DV0	Whole cooling season: 0:00–24:00	Weekdays: 8:00–18:00
Case GSDC-DV1	Weekdays: 0:00–24:00	Weekdays: 8:00–17:00
Case GSDC-DV2	Whole cooling season: 0:00–24:00	Weekdays: 8:00–17:00

load due to the equipment and occupancy changes from July 8 to 15. It can be seen that with the increase of the number of people and equipment, the load will increase. For each additional increment of 5 people and 5 computers, the total load will increase by 6.5 kW at most.

Figure **17** shows the comparison of indoor air temperature from July 23 to 30. When the number of indoor people and computers on each floor increases from 5 to 15, the indoor air temperature varies from 0.2˚C to 0.8˚C. When that increases by 20, the indoor air temperature varies around 1.5˚C. Note that the indoor air temperature can reach up to 30.2˚C, which significantly affects the thermal comfort, meaning that control measures should be taken. The control methods characterized by the changes of different water supply flow rates are proposed in Table **9**.

This optimized study chose the unfavourable case, which is an increment of 20 for people and computers. Table **10** presents the optimized results by increasing the water supply flow rate from July 22 to 27. The results show that when the flow rate increases by 20%, the indoor air temperature reaches up to 28˚C on July 22 and 23, while it stays below 26.5˚C on July 24 to 27. Considering the indoor thermal comfort and lower energy demand, a comprehensive control strategy and data analysis is acquired for further studies.

WEATHER-FORECAST-BASED PREDICTIVE CONTROLS

Operation Strategies for High-Temperature Weather Conditions

Solar radiation has the direct relationship with the outdoor air temperature. Therefore, it is necessary to account for the effect of outdoor air temperature and solar radiation on the building cooling and heating load. As shown in Figure **18** for the typical and predicted outdoor air temperatures, the temperature difference between the predicted year and the typical meteorological year is 2.0~5.0°C from August 5 to August 11. It should be noted that the current predicted condition was used as a real example to study the control strategies for different weather condition especially high temperature weather. The simulated air temperature was created in the predictive mode. The corresponding comparisons were conducted to determine the effective control strategy due to the changes of weather conditions.

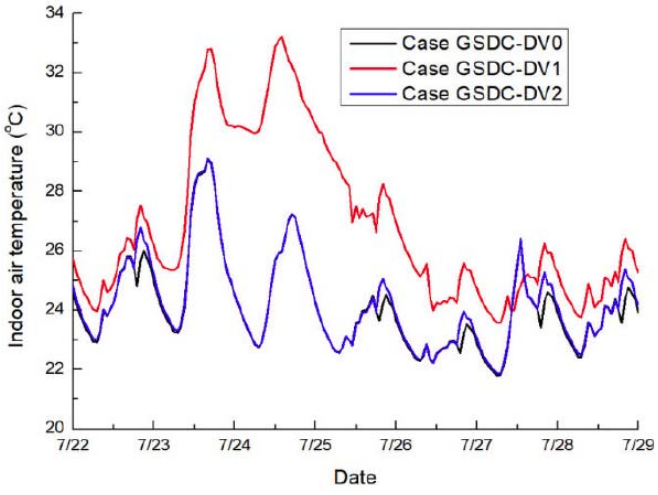

Figure 14: Comparison of indoor air temperature in GSDC-DV system.

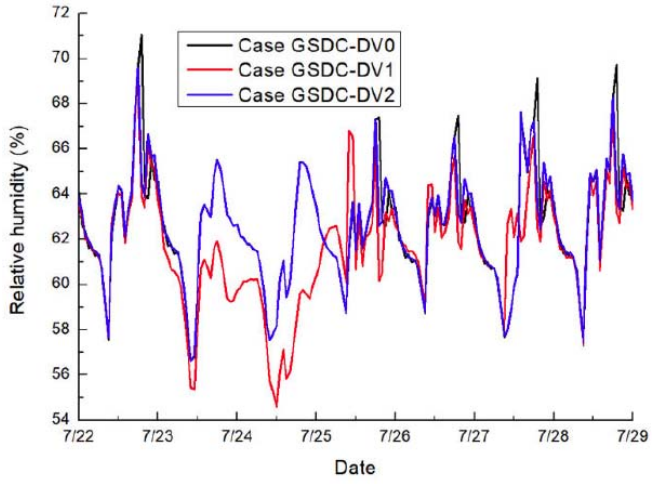

Figure 15: Comparison of indoor air humidity in GSDC-DV system.

Table 7: Comparison of Energy Consumption for Different Combined GSDC and DV System

Equipment	Rated power (kW)	Case GSDC-DV0 (kWh)	Case GSDC-DV1 (kWh)	Case GSDC-DV2 (kWh)
Pump in GSDC	2.2	4910.4	4910.4	3484.8
Pump in DV	0.44	3708.5	3308.3	3308.3
Heat pump unit	23.4	15024.8	15024.8	15024.8
Pump in GSHP	6.67	3521.8	3521.8	3521.8
Fan	2.38	6622.0	5907.4	5907.4
Total electric power	-	33787.4	32672.6	31247.0
Energy saving (%)	-	-	3.3	7.5

Table 8: Changes in the Number of People and Equipment

Original data	1st floor:10 people, 10 computers 2nd floor: 25 people,25 computers 3rd floor: 40 people,40 computers 4th floor: 30 people, 30 computers 5th floor: 15 people,15 computers
Prediction 1	Increment by 5 people and 5 computers on each floor
Prediction 2	Increment by 10 people and 10 computers on each floor
Prediction 3	Increment by 15 people and 15 computers on each floor
Prediction 4	Increment by 20 people and 20 computers on each floor

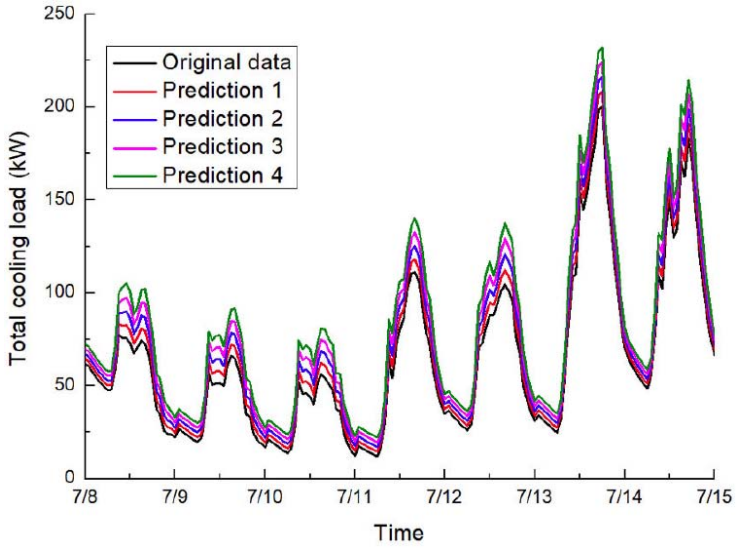

Figure 16: Comparison of cooling loads in five cases from July 8 to 15.

Figure **19** shows the indoor air temperature at each floor simulated from high-temperature weather conditions. Figure **20** shows the indoor air temperature obtained with an existing weather condition in which the typical meteorological year data in Jinan city was used. The results show that the maximum indoor air temperature from the existing weather data can reach up to 29.6°C. High temperature may cause indoor discomfort condition, therefore certain regulatory measures are required. Different control strategies were presented due to the high-temperature weather conditions. The common solution is to increase water supply flow rate and reduce the water supply temperature. Due to the high risk of condensation for

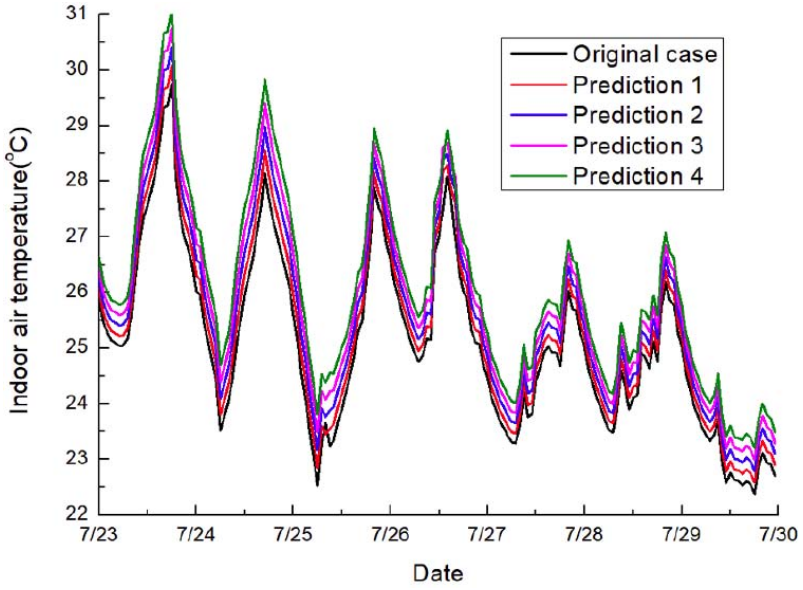

Figure 17: Comparison of indoor air temperature in five cases from July 23 to 30.

Table 9: Cases for Different Water Supply Flow Rates with an Increment of 20 People and 20 Computers

Case	Water supply flow rate changes
Case 0	No change
Case 1	Increment by 10%
Case 2	Increment by 15%
Case 3	Increment by 20%

Table 10: Maximum Indoor Air Temperature (˚C)

Case	July 22 to 23	July 24 to 27
Case 0	30.2	28.0
Case 1	29.2	27.3
Case 2	28.5	26.8
Case 3	28.0	26.4

the cooling floor, the temperature of water supply was kept larger than 16°C. Therefore, the main control strategy was to regulate the water supply flow rate.

The different control cases are proposed in Table **11**. The simulation results are presented for different high-temperature conditions shown in Figure **21**. The results showed that the control cases can reduce the air temperature by up to 1.0°C. To prevent the high economic cost of water pump, by analysing the results, indoor air temperature was maintained by increasing the water supply flow rate up to 25% on Monday.

Operation Strategies for Rainy Weather

In rainy weather, the outdoor air temperature is usually lower, and the indoor air temperature decreases accordingly, which results in the surplus of indoor cooling capacity. The simulation results of indoor air temperature in the existing weather data are shown in Figure **22**. Figure **23** shows the indoor air temperature in rainy weather is lower than that in the typical meteorological years. The predicted indoor air temperature is basically below 29.0˚C. Correspondingly, the control measures could be taken to reduce the operation cost under the condition that

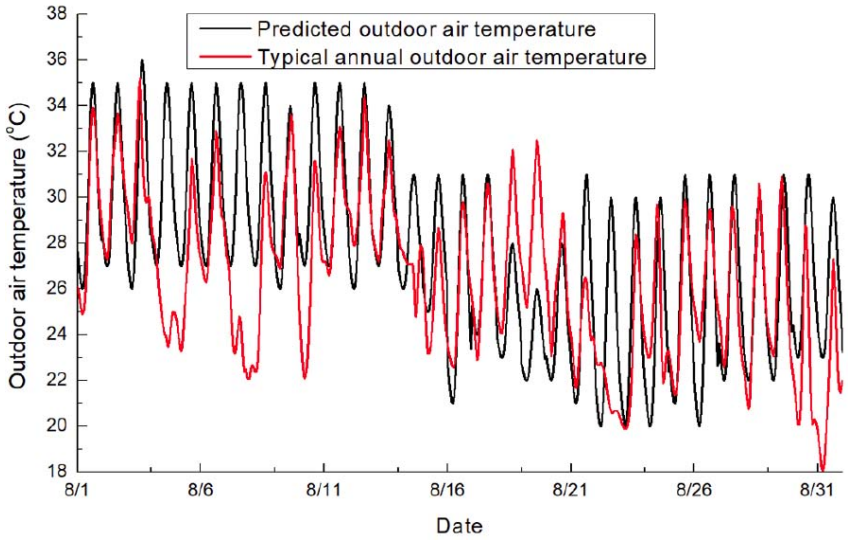

Figure 18: Hourly outdoor air temperatures from August 1 to 31.

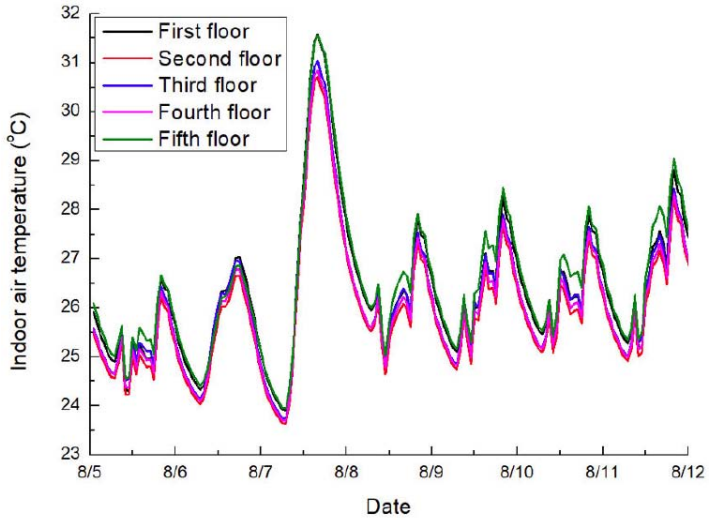

Figure 19: Indoor air temperature results on each floor obtained from high-temperature weather conditions (August 8: Monday).

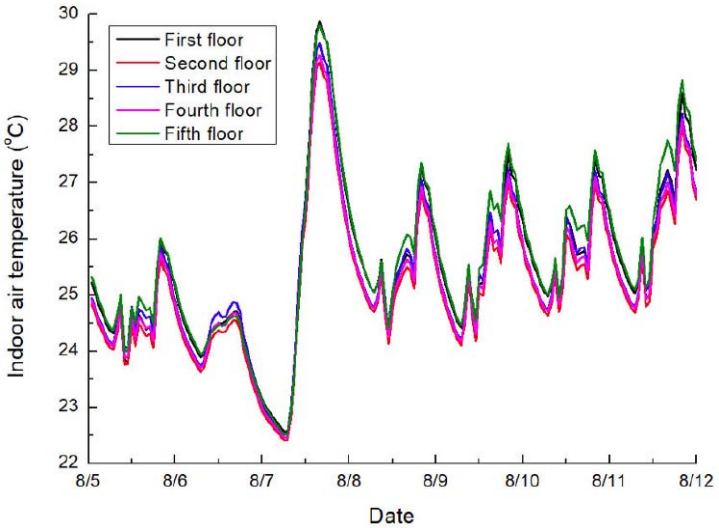

Figure 20: Indoor air temperature obtained from existing weather data (August 8: Monday).

the indoor air temperature and humidity meet the air-conditioning design standards. The control methods are proposed in Table **12**.

Table 11: Control Strategies for Different Water Supply Flow Rates Due to Predicted High-Temperature Weather

Case	Operation modes
hot0	Constant 30000 kg/h
hot1	Monday: increment of 20% at 8:00
hot2	Monday: increment of 25% at 8:00
hot3	Monday: increment of 30% at 8:00
hot4	Sunday: increment of 15% at 8:00
hot5	Sunday: increment of 20% at 8:00

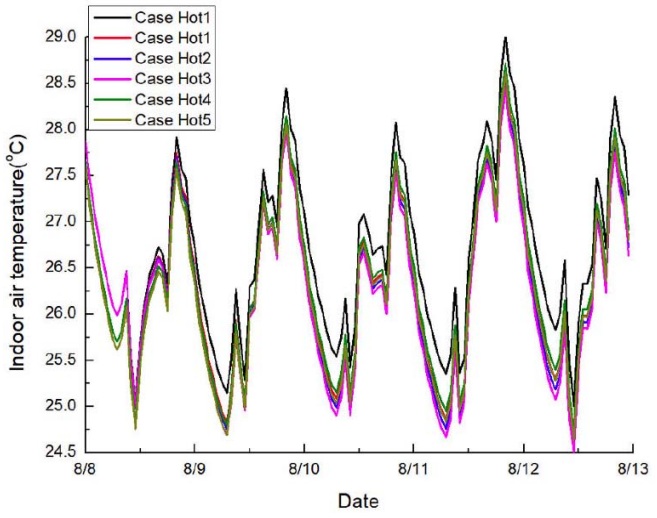

Figure 21: Comparison of indoor air temperature for the five optimized cases (August 8: Monday).

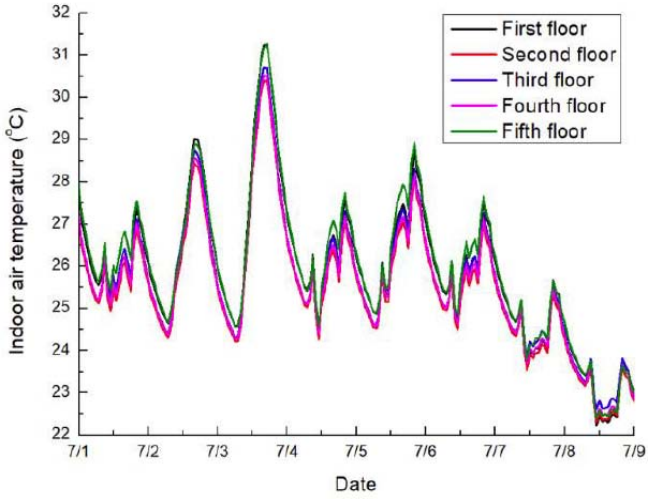

Figure 22: Indoor air temperature simulation results on each floor obtained with rainy weather.

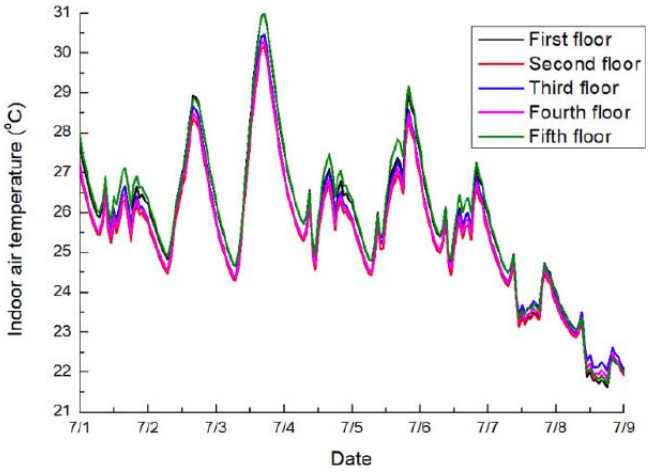

Figure 23: Indoor air temperature results on each floor obtained with typical existing weather.

Table 12: Control Strategies for Different Water Supply Flow Rates Due to Predicted Rainy Weather

Case	Modes
Rainy0	No change
Rainy1	Decrement by 10% at 8:00 on Monday
Rainy2	Decrement by 15% at 8:00 on Monday
Rainy3	Water supply flow rate remains unchanged, while the GSDC operates only on weekdays

The indoor air temperature simulation results for the three optimized cases are shown in Figure **24**. The indoor air temperature in Case Rainy2 increases within 0.3˚C, which is the minimum increase, basically meeting the air-conditioning design standards. Therefore, reducing 15% of water supply flow could be chosen as a control measure.

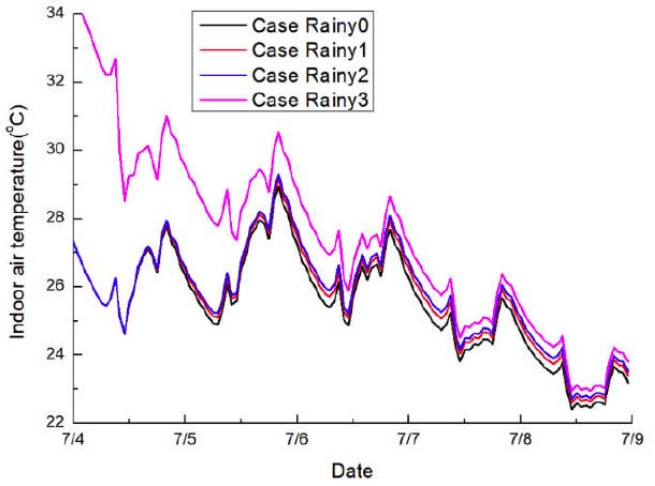

Figure 24: Comparison of indoor air temperature due to different water supply flow rates.

DISCUSSION

Based on the measured data from the monitoring system, people's mobility is actually high, and the load changes are dynamic. However, the people density in the simulation case was defined as a fixed value, which may cause the difference between the simulation results and the actual results. Field measurement should be extensively performed in the future to obtain the general regulations of people's mobility which can be applied to the simulation cases. The thermal comfort and energy saving potential of floor radiant air-conditioning systems are affected by many factors, such as the quantity and position of indoor furniture, window–wall ratio and floor material, etc. In the further studies, these factors should be taken into account to improve the control model, therefore enhancing the accuracy of the simulation.

CONCLUSIONS

This study utilized the TRNSYS program to study the control strategies of an RSFC–DV system. Intermittent operation and weather-forecast-based predictive control strategies were utilized to evaluate the indoor thermal environment conditions and the energy-saving potential. For the intermittent operation, one optimal operation scheme can., obtain the reduction of energy use by 3.3% for a schedule when the building was occupied every day, whereas an energy saving of up to 7.5% can be reached for a schedule when the building was shut off on weekends. For the operation strategies of equipment and occupancy changes, when the increment of load is less than 15% of the original load, there is no need to increase the water supply flow. Once the increment of load exceeds 15% or more of the original load, it is better to regulate the air conditioning system to meet the needs of indoor people. For the weather-forecast-based predictive control method, when the outdoor air temperature increases by 2.0~5.0˚C, an increase of 25% for the water supply flow rate can reduce the indoor air temperature by approximately 1.0˚C. When the outdoor temperature decreases by 2.0~6.0°C, a decrease of the water supply flow rate by 15% makes the indoor air temperature increase within 0.3˚C. The reduction of building energy consumption can be achieved by operating the intermittent control strategy, the cooling load variation can be regulated in advance when the weather-forecast-based control strategy was considered. In summary, the application of intermittent operation and weather-forecast-based control strategies can regulate the operation of radiant floor system and effectively reduce the building energy use.

CONFLICTS OF INTEREST

The authors declare no potential conflicts of interest with respect to the research, authorship, and/or publication of this article

ACKNOWLEDGEMENTS

This work was supported by the National Natural Science Foundation of China (51608310), Support plan for Outstanding Youth Innovation Team in Shandong Province (2019KJG005) and Science and Technology Plan Project of University in Shandong Province (J16LG07).

REFERENCES

[1] Liu J, Heidarinejad M, Gracik S, Srebric J. The impact of exterior surface convective heat transfer coefficients on the building energy consumption in urban neighborhoods with different plan area densities. Energy Build 2015; 86: 449-463. https://doi.org/10.1016/j.enbuild.2014.10.062

[2] Liu J, Heidarinejad M, Pitchurov G, Zhang L, Srebric J. An extensive comparison of modified zero-equation, standard k-ε, and LES models in predicting urban airflow. Sust Cities Soc 2018; 40: 28-43. https://doi.org/10.1016/j.scs.2018.03.010

[3] Gracik S, Heidarinejad M, Liu J, Srebric J. Effect of urban neighborhoods on the performance of building cooling systems. Build Environ 2015; 90: 15-29. https://doi.org/10.1016/j.buildenv.2015.02.037

[4] Heidarinejad M, Gracik S, Sadeghipour Roudsari M, Khoshdel Nikkho S, Liu J, Liu K, Pitchorov G, Srebric J. Influence of building surface solar irradiance on environmental temperatures in urban neighborhoods. Sust Cities Soc 2016; 26: 186-202. https://doi.org/10.1016/j.scs.2016.06.011

[5] Srebric J, Heidarinejad M, Liu J. Building neighborhood emerging properties and their impacts on multi-scale modeling of building energy and airflows. Build Environ 2015; 91: 246-262. https://doi.org/10.1016/j.buildenv.2015.02.031

[6] Khoshdel Nikkho S, Heidarinejad M, Liu J, Srebric J. Quantifying the impact of urban wind sheltering on the building energy consumption. Appl Therm Eng 2017; 116: 850-865. https://doi.org/10.1016/j.applthermaleng.2017.01.044

[7] Liu J, Heidarinejad M, Guo M, Srebric J. Numerical Evaluation of the Local Weather Data Impacts on Cooling Energy Use of Buildings in an Urban Area. Procedia Engineering 2015; 121: 381-388. https://doi.org/10.1016/j.proeng.2015.08.1082

[8] Zhang W, Zhang L, Cui P, Gao Y, Liu J, Yu M. The influence of groundwater seepage on the performance of ground source heat pump system with energy pile. Appl Therm Eng 2019; 162: 114217. https://doi.org/10.1016/j.applthermaleng.2019.114217

[9] Kong X-R, Deng Y, Li L, Gong W-S, Cao S-J. Experimental and numerical study on the thermal performance of ground source heat pump with a set of designed buried pipes. Appl Therm Eng 2017; 114: 110-117. https://doi.org/10.1016/j.applthermaleng.2016.11.176

[10] Villarino JI, Villarino A, Fernández FÁ. Experimental and modelling analysis of an office building HVAC system based in a ground-coupled heat pump and radiant floor. Applied Energy 2017; 190: 1020-1028. https://doi.org/10.1016/j.apenergy.2016.12.152

[11] Navarro L, de Gracia A, Colclough S, Browne M, McCormack SJ, Griffiths P, Cabeza LF. Thermal energy storage in building integrated thermal systems: A review. Part 1. active storage systems. Renewable Energy 2016; 88: 526-547. https://doi.org/10.1016/j.renene.2015.11.040

[12] Ito K, Inthavong K, Kurabuchi T, Ueda T, Endo T, Omori T, Ono H, Kato S, Sakai K, Suwa Y. CFD benchmark tests for indoor environmental problems: Part 4 air-conditioning airflows, residential kitchen airflows and fire-induced flow. International Journal of Architectural Engineering Technology 2015; 2(1): 76-102. https://doi.org/10.15377/2409-9821.2015.02.01.4

[13] Verbeke S, Audenaert A. Thermal inertia in buildings: A review of impacts across climate and building use. Renewable and Sustainable Energy Reviews 2018; 82: 2300-2318. https://doi.org/10.1016/j.rser.2017.08.083

[14] Zhang L, Liu J, Heidarinejad M, Kim MK, Srebric J. A Two-Dimensional Numerical Analysis for Thermal Performance of an Intermittently Operated Radiant Floor Heating System in a Transient External Climatic Condition. Heat Transf Eng 2019; 1-15. https://doi.org/10.1080/01457632.2019.1576422

[15] Roach P. Reducing the Cooling Energy of Existing Commercial Buildings with Passive Thermal Mass. International Journal of Architectural Engineering Technology 2017; 4(1): 1-10. https://doi.org/10.15377/2409-9821.2017.04.01.1

[16] Liu J, Dalgo DA, Zhu S, Li H, Zhang L, Srebric J. Performance analysis of a ductless personalized ventilation combined with radiant floor cooling system and displacement ventilation. Build Simul 2019; 12(5): 905-919. https://doi.org/10.1007/s12273-019-0521-9

[17] Kim MK, Liu J, Cao S-J. Energy analysis of a hybrid radiant cooling system under hot and humid climates: A case study at Shanghai in China. Build Environ 2018; 137: 208-214. https://doi.org/10.1016/j.buildenv.2018.04.006

[18] Shin MS, Rhee KN, Ryu SR, Yeo MS, Kim KW. Design of radiant floor heating panel in view of floor surface temperatures. Building and Environment 2015; 92: 559-577. https://doi.org/10.1016/j.buildenv.2015.05.006

[19] Liu J, Zhao Y, Li Z, Zhu S, Zhang L, Srebric J. Numerical evaluation of a Ductless Personalized Ventilation (DPV) combined with a radiant HVAC system: thermal comfort. IOP Conference Series: Materials Science and Engineering 2019; 609: 042031. https://doi.org/10.1088/1757-899X/609/4/042031

[20] Wu X, Olesen BW, Fang L, Zhao J, Wang F. Indoor temperatures for calculating room heat loss and heating capacity of radiant heating systems combined with mechanical ventilation systems. Energy Build 2016; 112: 141-148. https://doi.org/10.1016/j.enbuild.2015.12.005

[21] Zhang L, Huang X, Liang L, Liu J. Experimental study on heating characteristics and control strategies of ground source heat pump and radiant floor heating system in an office building, Procedia Engineering 2017; 205: 4060-4066. https://doi.org/10.1016/j.proeng.2017.09.890

[22] Ito K, Inthavong K, Kurabuchi T, Ueda T, Endo T, Omori T, Ono H, Kato S, Sakai K, Suwa Y. CFD benchmark tests for indoor environmental problems: Part 2 cross-ventilation airflows and floor heating systems. International Journal of Architectural Engineering Technology 2015; 2(1): 23-49. https://doi.org/10.15377/2409-9821.2015.02.01.2

[23] Ning B, Schiavon S, Bauman FS. A novel classification scheme for design and control of radiant system based on thermal response time. Energy Build 2017; 137: 38-45. https://doi.org/10.1016/j.enbuild.2016.12.013

[24] Sourbron M, De Herdt R, Van Reet T, Van Passel W, Baelmans M, Helsen L. Efficiently produced heat and cold is squandered by inappropriate control strategies: A case study. Energy and Buildings 2009; 41(10): 1091-1098. https://doi.org/10.1016/j.enbuild.2009.05.015

[25] Lehmann B, Dorer V, Gwerder M, Renggli F, Tödtli J. Thermally activated building systems (TABS): Energy efficiency as a function of control strategy, hydronic circuit topology and (cold) generation system. Applied Energy 2011; 88(1): 180-191. https://doi.org/10.1016/j.apenergy.2010.08.010

[26] Cen C, Jia Y, Liu K, Geng R. Experimental comparison of thermal comfort during cooling with a fan coil system and radiant floor system at varying space heights. Building and Environment 2018; 141: 71-79. https://doi.org/10.1016/j.buildenv.2018.05.057

[27] Romaní J, de Gracia A, Cabeza LF. Simulation and control of thermally activated building systems (TABS). Energy Build 2016; 127: 22-42. https://doi.org/10.1016/j.enbuild.2016.05.057

[28] Zhao K, Liu X-H, Jiang Y. Application of radiant floor cooling in large space buildings – A review. Renew Sust Energ Rev 2016; 55: 1083-1096. https://doi.org/10.1016/j.rser.2015.11.028

[29] Rhee K-N, Kim KW. A 50 year review of basic and applied research in radiant heating and cooling systems for the built environment. Build Environ 2015; 91: 166-190. https://doi.org/10.1016/j.buildenv.2015.03.040

[30] Shin M-S, Rhee K-N, Jung G-J. Optimal heating start and stop control based on the inferred occupancy schedule in a household with radiant floor heating system. Energy Build. 2020; 209: 109737. https://doi.org/10.1016/j.enbuild.2019.109737

[31] Lim J-H, Jo J-H, Kim Y-Y, Yeo M-S, Kim K-W. Application of the control methods for radiant floor cooling system in residential buildings. Build Environ 2006; 41(1): 60-73. https://doi.org/10.1016/j.buildenv.2005.01.019

[32] Rhee K-N, Olesen BW, Kim KW. Ten questions about radiant heating and cooling systems. Build Environ 2017; 112: 367-381. https://doi.org/10.1016/j.buildenv.2016.11.030

[33] Liu J, Xie X, Qin F, Song S, Lv D. A case study of ground source direct cooling system integrated with water storage tank system. Build Simul 2016; 9(6): 659-668. https://doi.org/10.1007/s12273-016-0297-0

[34] Zhang L, Li H, Liu J, Kim MK, Zhang L. Simulation and control of radiant floor cooling systems: intermittent operation and weather-forecast-based predictive controls. IOP Conference Series: Materials Science and Engineering 2019; 609: 062006. https://doi.org/10.1088/1757-899X/609/6/062006

[35] Liu J, Li Z, Kim MK, Zhu S, Zhang L, Srebric J. A comparison of the thermal comfort performances of a radiation floor cooling system when combined with a range of ventilation systems. Indoor Built Environ 2019; 1420326X19869412. https://doi.org/10.1177/1420326X19869412

[36] Liu J, Zhu S, Kim MK, Srebric J. A Review of CFD Analysis Methods for Personalized Ventilation (PV) in Indoor Built Environments. Sustainability 2019; 11(15): 4166. https://doi.org/10.3390/su11154166

[37] Shrivastava RL, Vinod K, Untawale SP. Modeling and simulation of solar water heater: A TRNSYS perspective. Renew Sust Energ Rev 2017; 67: 126-143. https://doi.org/10.1016/j.rser.2016.09.005

[38] De Carli M, Tonon M. Effect of modelling solar radiation on the cooling performance of radiant floors. Solar Energy 2011; 85(5): 689-712. https://doi.org/10.1016/j.solener.2010.12.012

[39] Pantelic J, Schiavon S, Ning B, Burdakis E, Raftery P, Bauman F. Full scale laboratory experiment on the cooling capacity of a radiant floor system. Energy and Buildings 2018; 170: 134-144. https://doi.org/10.1016/j.enbuild.2018.03.002

[40] Oubenmoh S, Allouhi A, Ait Mssad A, Saadani R, Kousksou T, Rahmoune M, Bentaleb M. Some particular design considerations for optimum utilization of under floor heating systems. Case Studies in Thermal Engineering 2018; 12: 423-432. https://doi.org/10.1016/j.csite.2018.05.010

[41] Cho SH, Zaheer-Uddin M. Predictive control of intermittently operated radiant floor heating systems. Energy Conv Manag 2003; 44(8): 1333-1342. https://doi.org/10.1016/S0196-8904(02)00116-4

[42] Macarthur JW, Mathur A, Zhao J. On-Line Recursive Estimation for Load Profile Prediction. ASHRAE Trans 1989; 26(1).

[43] Petersen S, Svendsen S. Method for simulating predictive control of building systems operation in the early stages of building design. Appl Energy 2011; 88(12): 4597-4606. https://doi.org/10.1016/j.apenergy.2011.05.053

[44] Kawashima M, Dorgan CE, Mitchell JW. Hourly thermal load prediction for the next 24 hours by ARIMA, EWMA, LR and an artificial neural network. ASHRAE Trans 1995; 101(1): 186-200.

[45] Wang D, Liu Y, Wang Y, Liu J. Numerical and experimental analysis of floor heat storage and release during an intermittent in-slab floor heating process. Applied Thermal Engineering 2014; 62(2): 398-406. https://doi.org/10.1016/j.applthermaleng.2013.09.028

[46] Jin HW. Study on Energy Saving from Intermittent Operation of Air-Conditioning System. Applied Mechanics and Materials 2014; 672-674: 542-545. https://doi.org/10.4028/www.scientific.net/AMM.672-674.542

[47] Li Q-Q, Chen C, Zhang Y, Lin J, Ling H-S, Ma Y. Analytical solution for heat transfer in a multilayer floor of a radiant floor system. Building Simulation 2014; 7(3): 207-216. https://doi.org/10.1007/s12273-013-0152-5

Received on 15-12-2019 Accepted on 30-12-2019 Published on 31-12-2019

DOI: http://dx.doi.org/10.15377/2409-9821.2019.06.5